FEBS Letters 583 (2009) 1121–1126

journal homepage: www.FEBSLetters.org

Effect of ε subunit on the rotation of thermophilic *Bacillus* F_1-ATPase

Masato Tsumuraya [a], Shou Furuike [b], Kengo Adachi [b], Kazuhiko Kinosita Jr. [b], Masasuke Yoshida [a,c,*]

[a] *Chemical Resources Laboratory, Tokyo Institute of Technology, Nagatsuta 4259, Yokohama 226-8503, Japan*
[b] *Department of Physics, Faculty of Science and Engineering, Waseda University, Shinjuku-ku, Tokyo 169-8555, Japan*
[c] *ICORP ATP Synthesis Regulation Project, Japan Science and Technology Corporation (JST), Aomi 2-41, Tokyo 135-0064, Japan*

ARTICLE INFO

Article history:
Received 7 February 2009
Revised 24 February 2009
Accepted 26 February 2009
Available online 4 March 2009

Edited by Peter Brzezinski

Keywords:
F_1, F_1-ATPase
ATP synthase
Motor
Single-molecule
Epsilon subunit

ABSTRACT

F_1-ATPase is an ATP-driven motor in which γε rotates in the $\alpha_3\beta_3$-cylinder. It is attenuated by MgADP inhibition and by the ε subunit in an inhibitory form. The non-inhibitory form of ε subunit of thermophilic *Bacillus* PS3 F_1-ATPase is stabilized by ATP-binding with micromolar K_d at 25 °C. Here, we show that at [ATP] > 2 μM, ε does not affect rotation of PS3 F_1-ATPase but, at 200 nM ATP, ε prolongs the pause of rotation caused by MgADP inhibition while the frequency of the pause is unchanged. It appears that ε undergoes reversible transition to the inhibitory form at [ATP] below K_d.

1. Introduction

F_1 is a water soluble portion of ATP synthase (F_oF_1) that catalyzes synthesis of ATP [1,2]. The simplest F_1 from bacteria, such as *Escherichia coli* (EF_1) and thermophilic *Bacillus* PS3 (TF_1), has a subunit composition of $\alpha_3\beta_3\gamma\delta\varepsilon$. F_1 is an ATP-driven rotary motor in which γ rotates in the $\alpha_3\beta_3$-cylinder [3,4]. Starting from γ angle at 0° (ATP-waiting dwell), ATP-binding induces the 80°-substep rotation of γ, the ATP previously bound is hydrolyzed (catalytic dwell), and Pi-release induces 40°-substep rotation [5–8]. Duration of ATP-waiting dwell is inversely proportional to [ATP] but that of catalytic dwell is independent from [ATP], always few milliseconds.

ATP synthase can catalyze a back reaction, ATP hydrolysis. When a cell is starved and ATP production has ceased, wasteful ATP hydrolysis by ATP synthase should be avoided by the regulatory mechanisms that respond to the change of cellular energy level, typically cellular [ATP] and [ADP] (and [AMP] as well). Actual physiological significance is yet unclear but several mechanisms that inhibit ATPase activity of F_1 and ATP synthase have been known. A common mechanism observed for F_1 from most organisms is "MgADP inhibition" in which occasional persistent occupation of a catalytic site of β by MgADP prevents further catalytic turnover of ATP hydrolysis [9–11]. In a single molecule observation, regular rotation of $\alpha_3\beta_3\gamma$ complex of TF_1, which continues several tens of seconds, pauses at 80° when the enzyme lapses into MgADP inhibition, and resumes after several tens of seconds [11]. The $\alpha_3\beta_3\gamma$ shows initial burst of ATP hydrolysis when ATP is added, but MgADP inhibition gradually progresses, reaching dynamic equilibrium between active and MgADP-inhibited state that defines the steady-state ATPase activity [11,12]. This situation makes interpretation for apparent values of K_m and V_{max} of the steady-state ATPase activity very complicated.

Another regulatory mechanism involves ε subunit that associates with γ and constitutes a rotor assembly in F_1 [13–18]. The ε subunit is composed of two domains [19]; N-terminal β-sandwich domain, by which ε binds to globular domain of γ, and C-terminal domain with two α-helices, which undergoes extension-hairpin transition [20–22]. ATPase activity is inhibited only when two helices extend [23]. ATP binds to and stabilizes the non-inhibitory hairpin form of isolated ε of TF_1 with micromolar K_d at 25 °C [24,25]. ATPase activity of $\alpha_3\beta_3\gamma\varepsilon$ complex of TF_1 starts with an initial lag that is gradually activated to reach a steady-state rate [17]. The transition of ε from inhibitory to non-inhibitory form is largely responsible for this activation [26]. At [ATP] > 0.1 mM, the transition is complete and steady-state ATPase activity of $\alpha_3\beta_3\gamma\varepsilon$ reaches the same level as $\alpha_3\beta_3\gamma$ [17,26]. Thus, despite very different initial ATPase activity of $\alpha_3\beta_3\gamma$ (burst) and $\alpha_3\beta_3\gamma\varepsilon$ (lag), steady-state

* Corresponding author. Address: Chemical Resources Laboratory, Tokyo Institute of Technology, Nagatsuta 4259, Yokohama 226-8503, Japan. Fax: +81 45 924 5277.
E-mail address: myoshida@res.titech.ac.jp (M. Yoshida).

0014-5793/$36.00
doi:10.1016/j.febslet.2009.02.038

ATPase activity, as well as rotation, of $\alpha_3\beta_3\gamma$ and $\alpha_3\beta_3\gamma\varepsilon$ are the same at [ATP] > 0.1 mM where ε in $\alpha_3\beta_3\gamma\varepsilon$ is stabilized in the non-inhibitory form by ATP-binding. Here, we extend the study to sub-micromolar ATP range where ATP no longer can bind to ε.

2. Materials and methods

2.1. Proteins

Plasmids for expression of $\alpha_3\beta_3\gamma\varepsilon$, $\alpha_3\beta_3\gamma\varepsilon^{\Delta C}$ (containing a stop codon after ε-D87) and $\alpha_3\beta_3\gamma$ complexes derived from thermophilic *Bacillus* PS3 carrying mutations of α-C193S, His_{10}-tag at N-terminus of β, ε-I47C and ε-D73C (for $\alpha_3\beta_3\gamma\varepsilon$ and $\alpha_3\beta_3\gamma\varepsilon^{\Delta C}$), or γ-S107C and γ-I210C (for $\alpha_3\beta_3\gamma$), were introduced into *E. coli* strain JM103Δ*unc*B-D. The expressed complexes were purified as described [27].

2.2. ATPase activity

ATPase activity was measured at 25 °C by an ATP regenerating coupling assay monitored by NADH oxidation at 340 nm [7]. The reaction was initiated by adding enzyme into the assay solution (1.2 ml) containing indicated amount of Mg–ATP (1:1 mixture of $MgCl_2$ and ATP). ATP hydrolysis by $\alpha_3\beta_3\gamma$ and $\alpha_3\beta_3\gamma\varepsilon^{\Delta C}$ started with an initial rapid phase and then reached the steady-state activity. The activities at final 150 s (2 mM ATP), 200 s (600 μM, 200 μM ATP) or 600 s ([ATP] < 60 μM) were taken as the steady-state activities. In the case of $\alpha_3\beta_3\gamma\varepsilon$, ATP hydrolysis at low [ATP] started with a very long initial lag and therefore the activity below 60 μM ATP was measured as follows. The $\alpha_3\beta_3\gamma\varepsilon$ was preincubated at 25 °C in Mg–ATP at a concentration 120-fold of the final one, 2.5 mM phosphoenolpyruvate, 0.2 mg ml^{-1} pyruvate kinase, 5 mM $MgCl_2$, 100 mM potassium phosphate, pH 7.5, 100 mM KCl, 2 mM EDTA for 5 min (final [ATP] 60 μM), 10 min (20 μM), 15 min (6 μM), 20 min (2 μM), 25 min (600 nM), or 35 min (200 nM). The mixture (10 μl) was added to 1.2 ml of the assay mixture. Steady-state activity was defined by NADH oxidation rate between 0 s and 500 s ([ATP] ⩾ 2 μM) or between 0 s and 400 s ([ATP] ⩽ 600 nm) after initiation of the reaction. In another series of experiments at 200 nM, 600 nM and 2 μM ATP, 10-fold molar excess of isolated ε (relative to $\alpha_3\beta_3\gamma$) was added to the mixture in which $\alpha_3\beta_3\gamma$ was catalyzing steady-state ATP hydrolysis and the activity (0–400 s after the time point of addition of ε) with and without addition of ε was compared.

2.3. Observation of rotation

Two cysteines (ε-I47C, ε-D73C) in $\alpha_3\beta_3\gamma\varepsilon$ and $\alpha_3\beta_3\gamma\varepsilon^{\Delta C}$ were biotinylated by incubation with 5-fold molar excess of 6-{*N*′-[2-(*N*-maleimido)ethyl]-*N*-piperazinylamido}hexyl-D-biotinamide (Dojindo, Kumamoto, Japan) for 2 h at room temperature, and unbound biotins were removed by a PD10 column (GE Healthcare, UK). Setup for observing system and observation of rotation are described in Supplement.

3. Results

3.1. Steady-state ATPase activity

Steady-state ATPase activities of $\alpha_3\beta_3\gamma$ and $\alpha_3\beta_3\gamma\varepsilon$ in bulk solution were measured. Also examined was $\alpha_3\beta_3\gamma\varepsilon^{\Delta C}$ in which $\varepsilon^{\Delta C}$ lacks C-terminal helices and ability to bind ATP. ATPase activities of $\alpha_3\beta_3\gamma$ and $\alpha_3\beta_3\gamma\varepsilon^{\Delta C}$ started with initial burst at almost the same velocities at all [ATP] (data not shown). The activity was rapidly slowed down as MgADP inhibition progressed. ATPase activity of $\alpha_3\beta_3\gamma\varepsilon$ started with a slow lag phase [17]. In the purified $\alpha_3\beta_3\gamma\varepsilon$, ε adopts an inhibitory form, and the recovery from initial lag reflects the transition of ε from the extended to hairpin form [26]. This lag phase becomes long as [ATP] decreases [17]. To avoid a long initial lag phase of $\alpha_3\beta_3\gamma\varepsilon$ at low [ATP], we preincubated $\alpha_3\beta_3\gamma\varepsilon$ with high [ATP] in the presence of an ATP-regenerating system and diluted it into the reaction mixture to give the final [ATP]. With these cautions, data of steady-state ATPase activities of $\alpha_3\beta_3\gamma\varepsilon$, $\alpha_3\beta_3\gamma\varepsilon^{\Delta C}$ and $\alpha_3\beta_3\gamma$ were collected. Remarkably, although the initial phases were very different, steady-state ATPase activities of $\alpha_3\beta_3\gamma\varepsilon$, $\alpha_3\beta_3\gamma\varepsilon^{\Delta C}$ and $\alpha_3\beta_3\gamma$ were very similar at [ATP] > 2 μM (Fig. 1A). Since the steady-state activity is mostly determined by the dynamic equilibrium between active and MgADP-inhibited state, ε does not seem to have significant effect on this equilibrium at this [ATP] range. Below 2 μM ATP, the steady-state activity of $\alpha_3\beta_3\gamma\varepsilon^{\Delta C}$ and $\alpha_3\beta_3\gamma$ decreased in proportion to the decrease in [ATP], but the steady-state activity of $\alpha_3\beta_3\gamma\varepsilon$ decreased more sharply (Fig. 1A, *inset*). At 600 nM ATP, the steady-state activity of $\alpha_3\beta_3\gamma\varepsilon$ was ~40% of $\alpha_3\beta_3\gamma\varepsilon^{\Delta C}$, and at 200 nM ATP, it became barely detectable level. Consistently, when excess amount of isolated ε was added to the $\alpha_3\beta_3\gamma$ catalyzing the steady-state ATP hydrolysis at 2 μM, 600 nM and 200 nM ATP, activity at 2 μM ATP was unchanged but activities at 600 nM and 200 nM ATP were slowed down to ~70% and ~20%, respectively (Fig. 1B, *inset*). Thus, the effect of C-terminal helical domain of ε on the steady-state ATPase activity is evident only at sub-micromolar [ATP]. Because initial and steady-state ATPase activities of $\alpha_3\beta_3\gamma\varepsilon^{\Delta C}$ were similar to those of $\alpha_3\beta_3\gamma$ at all [ATP], the N-terminal domain of ε has minimum effect on enzyme kinetics of $\alpha_3\beta_3\gamma$.

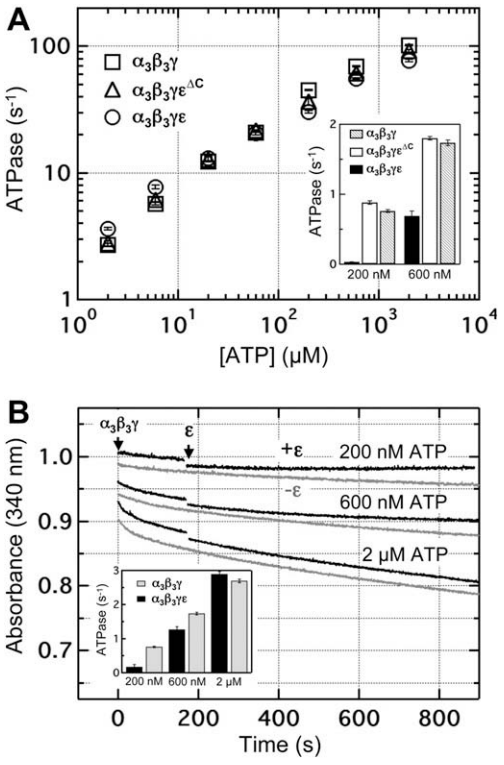

Fig. 1. (A) Steady-state ATP hydrolysis rates by $\alpha_3\beta_3\gamma\varepsilon$, $\alpha_3\beta_3\gamma\varepsilon^{\Delta C}$ and $\alpha_3\beta_3\gamma$. Measurement and definition of the steady-state hydrolysis activity are described in Section 2. *Inset*; steady-state ATP hydrolysis rates below 1 μM ATP. (B) Trace of ATP hydrolysis activities of $\alpha_3\beta_3\gamma$ at 200 nM, 600 nM, and 2 μM ATP. Excess amount of ε was added as indicated. *Inset*; comparison of ATP hydrolysis rates with and without addition of ε.

3.2. Observation of rotating molecules for several seconds

We observed the rotation of $\alpha_3\beta_3\gamma\varepsilon$ and $\alpha_3\beta_3\gamma\varepsilon^{\Delta C}$ at various [ATP] in a short time-scale (2–8 s) under dark-field illumination on a fast-framing camera (8000 frames s^{-1}). In either case, rotation was probed by a 40-nm bead attached to the β-sandwich region of ε through biotinylated residues (ε-I47C, ε-D73C), rather than γ, to avoid a possible mistaken observation of rotation of the ε-less complex. The viscous friction derived from the 40-nm bead is small enough to observe the rotation without load at this framing speed [5]. Below 2 μM ATP only very few rotating molecules of $\alpha_3\beta_3\gamma\varepsilon$ were found and we improved this by preincubation of biotinylated

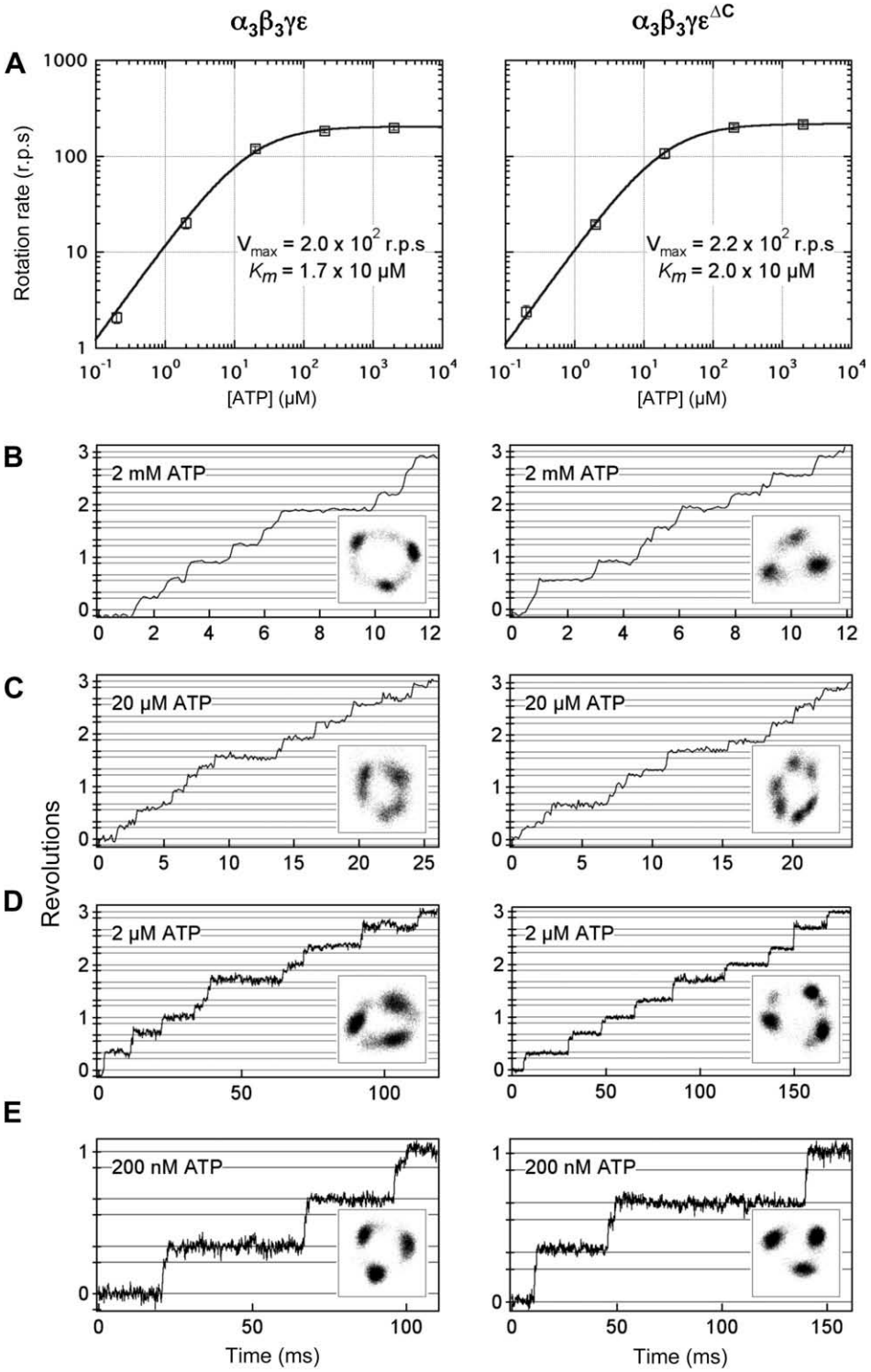

Fig. 2. Rotation of 40 nm-beads attached to ε (or $\varepsilon^{\Delta C}$) of $\alpha_3\beta_3\gamma\varepsilon$ and $\alpha_3\beta_3\gamma\varepsilon^{\Delta C}$ observed for several seconds with a fast-framing camera. (A) [ATP] dependence of rotation speed. (B–E) Time courses of stepping rotation at indicated [ATP]. The time courses shown in (E) were not typical time segments but those happened to contain short ATP-waiting dwells. Horizontal gray lines indicate 0°-position and 80°-positions in a 120°-unit rotation. *Insets*, centroid position of beads. Experimental details are described in Section 2.

$\alpha_3\beta_3\gamma\varepsilon$ with high [ATP] in the presence of an ATP-regenerating system before dilution to the final [ATP] [27]. All observed rotations were counterclockwise. The rotation rates of $\alpha_3\beta_3\gamma\varepsilon$ and $\alpha_3\beta_3\gamma\varepsilon^{\Delta C}$ averaged over ~1 s were very similar each other at all [ATP] ranging 200 nM to 2 mM (Fig. 2A) and can be fitted well with a simple Michaelis–Menten kinetics with V_{max} = 200 revolution s^{-1} and K_m = 17 μM for $\alpha_3\beta_3\gamma\varepsilon$ and V_{max} = 220 revolution s^{-1} and K_m = 20 μM for $\alpha_3\beta_3\gamma\varepsilon^{\Delta C}$. These values are also very close to those of $\alpha_3\beta_3\gamma$ [5,8]. Both $\alpha_3\beta_3\gamma\varepsilon$ and $\alpha_3\beta_3\gamma\varepsilon^{\Delta C}$ exhibited stepping rotation that was similar to $\alpha_3\beta_3\gamma$. At 2 mM ATP, only the catalytic dwell was observed since ATP-waiting dwell was too short (Fig. 2B). At 20 μM (~K_m) ATP, both ATP-waiting dwell at 0° and catalytic dwell at 80° with nearly equal durations repeated in every 120°-unit rotation (Fig. 2C). At 2 μM ATP, ATP-waiting dwell became longer than catalytic dwell (Fig. 2D). At 200 nM ATP, catalytic dwell was barely visible (Fig. 2E). Analysis of the duration histogram of the catalytic dwells at different [ATP] (Supplementary, Fig. S1A–C) showed that two sequential catalytic reactions occurred during the catalytic dwell, of which averaged rate constants were $k_1 = 8.6 \times 10^2\ s^{-1}$ and $k_2 = 7.6 \times 10^3\ s^{-1}$ for $\alpha_3\beta_3\gamma\varepsilon$ and $k_1 = 9.0 \times 10^2\ s^{-1}$ and $k_2 = 7.3 \times 10^3\ s^{-1}$ for $\alpha_3\beta_3\gamma\varepsilon^{\Delta C}$. These values are close to those of $\alpha_3\beta_3\gamma$ ($k_1 = 7.5 \times 10^2\ s^{-1}$ and $k_2 = 8.6 \times 10^3\ s^{-1}$) [8]. Therefore, the presence of ε (and $\varepsilon^{\Delta C}$ as well) in F_1 does not have significant effect on catalytic events occurring in catalytic dwell, namely ATP-hydrolysis and Pi-release [7,8]. Apparent ATP-binding rates were obtained from the analysis of duration histograms of ATP-waiting dwells at 2 μM and 200 nM ATP (Supplementary, Fig. S1D and E). These histograms could be fitted by a single-reaction scheme and the ATP-binding rate constants were calculated to be $3.8 \times 10^7\ M^{-1}\ s^{-1}$ for $\alpha_3\beta_3\gamma\varepsilon$ and $3.6 \times 10^7\ M^{-1}\ s^{-1}$ for $\alpha_3\beta_3\gamma\varepsilon^{\Delta C}$. These values are in the same range of $\alpha_3\beta_3\gamma$ ($2–3 \times 10^7\ M^{-1}\ s^{-1}$) [5,8]. To summarize, as far as we observed actively rotating molecules of $\alpha_3\beta_3\gamma\varepsilon$ and $\alpha_3\beta_3\gamma\varepsilon^{\Delta C}$ by a fast-framing camera for short period, their rotation kinetics are very similar to those of $\alpha_3\beta_3\gamma$ at all [ATP] ranging 200 nM–2 mM and effect of the presence of ε in the complex is very little if any.

3.3. Observation of rotation for several tens of minutes

Next, we observed rotation for long period. A 40-nm bead and fast-framing CCD camera were not suitable for long (up to 2 h) observation because of limitation of computational memory

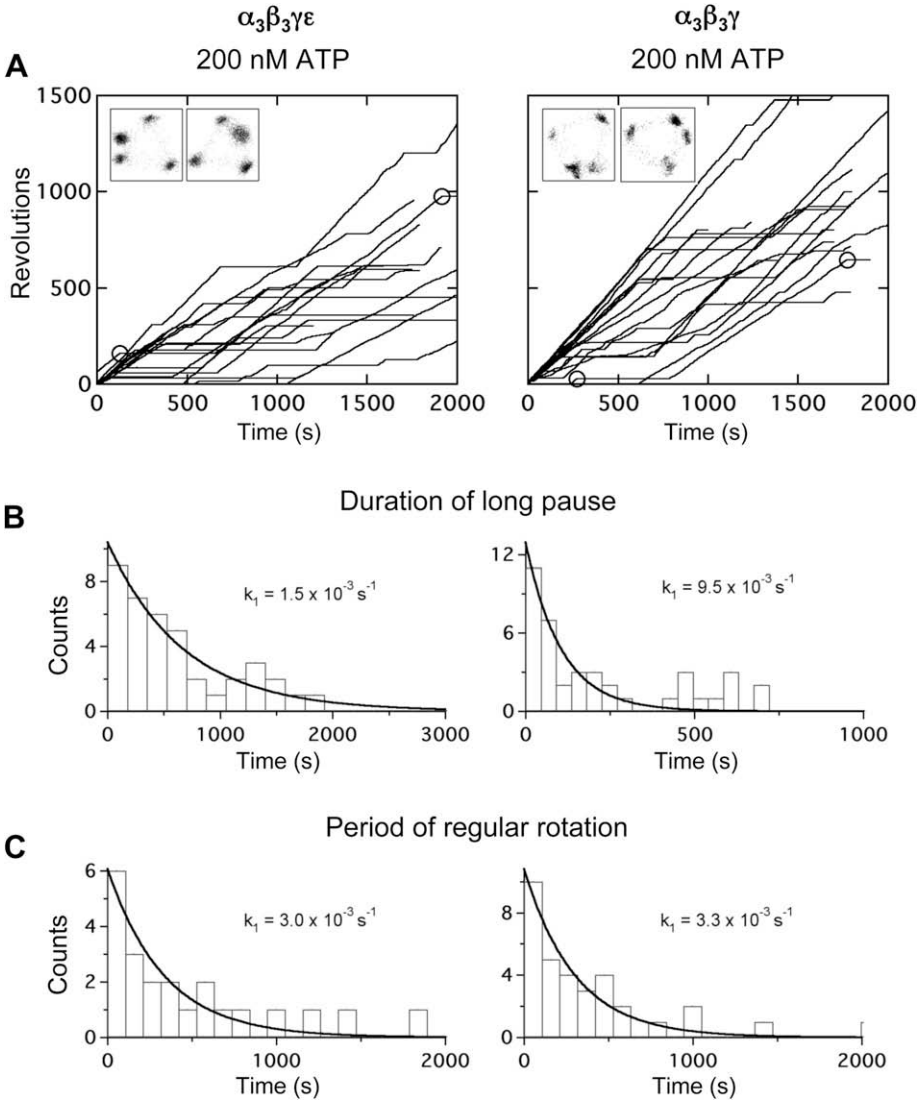

Fig. 3. Rotation of duplex 200-nm beads attached to ε of $\alpha_3\beta_3\gamma\varepsilon$ or to γ of $\alpha_3\beta_3\gamma$ in 200 nM ATP observed for several tens of minutes. (A) Time-courses of rotation. *Insets*, centroid positions of beads in the segments indicated circle in the trajectory. Insets: The positions of three ATP-waiting dwells and long pauses (indicated by the circles) of the same rotating bead are shown. (B) Histogram of pause duration at 80°. Pauses at 80° that were longer than 10 s were collected and analyzed. (C) Histogram of period of regular rotation between one pause (>10 s) and next pause (>10 s). Solid lines are the simulated curves with a single exponential equation, constant × exp(−*kt*).

capacity. Instead, we attached polystyrene bead of 200-nm diameter to ε of $\alpha_3\beta_3\gamma\varepsilon$ and observed rotation at 30 frames s^{-1} (200 nM ATP) or at 150 frames s^{-1} (2 mM ATP). The catalytic dwell at 80° after ATP-waiting dwell was no longer observable because of slow temporal resolution of the camera and of the slow stepping motion by viscous load imposed on rotating 200-nm beads. We chose rotating $\alpha_3\beta_3\gamma\varepsilon$ that happened to bind duplex beads, which showed clearer rotation than a single bead. In the case of $\alpha_3\beta_3\gamma\varepsilon^{\Delta C}$, rotating polystyrene beads were shortly detached from the complex probably together with $\varepsilon^{\Delta C}$, from the complex shortly, possibly because viscous load might break weakened association between $\varepsilon^{\Delta C}$ and γ. Therefore, we were obliged to use $\alpha_3\beta_3\gamma$ with polystyrene beads attached on γ, given that bulk-phase activity of $\alpha_3\beta_3\gamma\varepsilon^{\Delta C}$ are the same to that of $\alpha_3\beta_3\gamma$. At 2 mM ATP, $\alpha_3\beta_3\gamma\varepsilon$ repeated two phases, *i.e.*, continuous regular rotations and long pauses, and their life-times (a reciprocal of rate constant, τ) were 33 s and 28 s, respectively (data not shown). Under the same conditions, $\alpha_3\beta_3\gamma$ also showed very similar rotation characteristics with life-times of 22 s for regular rotation and 32 s for long pause [11]. Since the long pause of $\alpha_3\beta_3\gamma$ was previously assigned to be due to MgADP inhibition, the above observation indicates that ε does not have effect on the MgADP inhibition at high ATP.

At 200 nM ATP, regular rotation was also interrupted by long pauses (Fig. 3A). ATP-waiting dwells were seen at every 120° with averaged dwelling time of ~0.2 s for both $\alpha_3\beta_3\gamma\varepsilon$ and $\alpha_3\beta_3\gamma$, and the positions of the long pauses were always at ~80° after the ATP-waiting dwells (Fig. 3A, *inset*). We collected the data from all pauses at 80° longer than 10 s. The duration histogram of the 80°-pause was fitted with a single-reaction scheme assuming transition of inactive state (long pause) to active state (regular rotation) (Fig. 3B). The rate constants were estimated to be $1.5 \times 10^{-3}\ s^{-1}$ for $\alpha_3\beta_3\gamma\varepsilon$ and $9.5 \times 10^{-3}\ s^{-1}$ for $\alpha_3\beta_3\gamma$. Therefore, life-time of the pause of $\alpha_3\beta_3\gamma\varepsilon$, 670 s, was 6-fold longer than that of $\alpha_3\beta_3\gamma$, 110 s. Also, the periods of contiguous regular rotation between one long pause (>10 s) and the next long pause (>10 s) were collected and analyzed. In both $\alpha_3\beta_3\gamma\varepsilon$ and $\alpha_3\beta_3\gamma$, the histogram could be fitted with a single-reaction scheme assuming transition from active state (regular rotation) to inactive state (long pause) (Fig. 3C). The rate constants of the transitions were estimated to be $3.0 \times 10^{-3}\ s^{-1}$ for $\alpha_3\beta_3\gamma\varepsilon$ and $3.3 \times 10^{-3}\ s^{-1}$ for $\alpha_3\beta_3\gamma$. Thus, life-time of the active state of $\alpha_3\beta_3\gamma\varepsilon$ (330 s), in which regular rotation continues, is similar to that of $\alpha_3\beta_3\gamma$ (300 s). These results suggest that ε does not increase the frequency of incidence of at 80°-pause but, once the regular rotation is lapsed into the pause, it prolongs the pausing duration 6-fold.

4. Discussion

We found here that as far as we analyzed actively rotating $\alpha_3\beta_3\gamma\varepsilon$ molecules for several seconds, there was no obvious difference in rotation kinetics between $\alpha_3\beta_3\gamma\varepsilon$ and $\alpha_3\beta_3\gamma\varepsilon^{\Delta C}$ (and $\alpha_3\beta_3\gamma$) at any [ATP] tested. Rate constants of ATP binding ($2–4 \times 10^7\ M^{-1}\ s^{-1}$) and those of two events in the catalytic dwell ($k_1 = 7–9 \times 10^2\ s^{-1}$, $k_2 = 7–9 \times 10^3\ s^{-1}$) are all similar among these complexes. This result is not surprising because C-terminal helices of ε in rotating $\alpha_3\beta_3\gamma\varepsilon$ molecule should be folded in the non-inhibitory hairpin conformation and ε does not have any contact with $\alpha_3\beta_3$-cylinder part that is driving catalysis and rotation.

When we observed rotating molecules as long as several tens of minutes, we noticed that long pauses at 80°-position interrupted the continuous regular rotation. Our observations are summarized and explained by a model shown in Fig. 4. At 2 mM ATP, period of the regular rotation ($\tau = 20–30$ s) and duration of long pause ($\tau = \sim 30$ s) are common to $\alpha_3\beta_3\gamma\varepsilon$ and $\alpha_3\beta_3\gamma$ (Fig. 4A). However, the effect of ε becomes evident at sub-micromolar [ATP] where

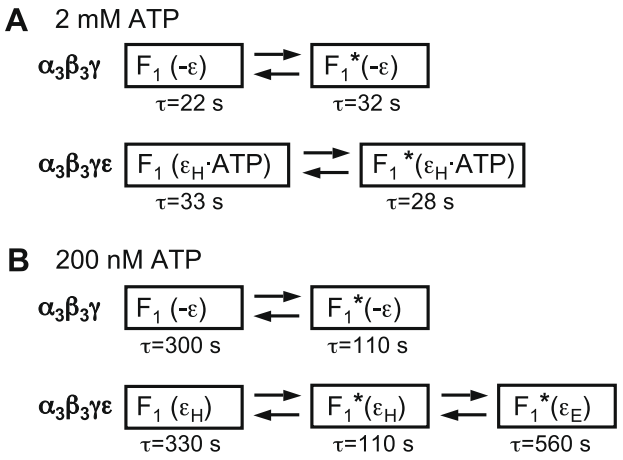

Fig. 4. A model for the transition of ε subunit in F_1 catalyzing steady-state ATP hydrolysis. Symbols are; $F_1(-\varepsilon)$, F_1 lacking ε subunit; F_1^*, F_1 in MgADP-inhibited state; ε_H, ε in hairpin form; ε_H·ATP, ε_H stabilized by ATP-binding; ε_E, ε in extended form; τ, life-time. (A) At 2 mM ATP, ε_H is stabilized by ATP-binding and τ of $F_1^*(\varepsilon_H\cdot ATP)$ is similar to that of $F_1^*(-\varepsilon)$. Actually, ε has no effect on steady-state ATPase activity at high [ATP]. (B) At 200 nM ATP, τ of active F_1 is similar between $F_1(-\varepsilon)$ and $F_1(\varepsilon_H)$. ε_H might not bind ATP. Likewise, τ of inactive F_1^* is assumed to be similar between $F_1^*(-\varepsilon)$ and $F_1^*(\varepsilon_H)$. The ε subunit in $F_1^*(\varepsilon_H)$ can change its conformation into an extended form, $F_1^*(\varepsilon_H)$, that has longer τ than $F_1^*(\varepsilon_H)$ and $F_1^*(-\varepsilon)$.

long pause of $\alpha_3\beta_3\gamma\varepsilon$ ($\tau = 670$ s) is 6-fold longer than that of $\alpha_3\beta_3\gamma$ ($\tau = 110$ s) (Fig. 4B). During the prolonged pauses, C-terminal helices of ε in $\alpha_3\beta_3\gamma\varepsilon$ are supposed to be inhibitory extended form and can interact with catalytic $\alpha_3\beta_3$-cylinder. Interestingly, frequency of the incidence of the pauses of $\alpha_3\beta_3\gamma\varepsilon$, expressed as the life-time of actively rotating species of molecules ($\tau = 330$ s), was actually very similar to those of $\alpha_3\beta_3\gamma$ ($\tau = 300$ s). Therefore, the effect of ε is not to interrupt the regular rotation but to prolong the pause duration. Taking into account that K_d value of ATP-binding to the isolated ε in the hairpin form is in the range of micromolar [ATP] at 25 °C [26], a simple explanation for the above observations is as follows. At [ATP] higher than micromolar, ATP binds and stabilizes ε in $\alpha_3\beta_3\gamma\varepsilon$ in non-inhibitory hairpin form and the transition to inhibitory extended form is prevented. At sub-micromolar [ATP], ATP can no longer bind and stabilize the non-inhibitory hairpin form of ε and reversible transition from non-inhibitory to inhibitory form becomes allowed. A possibility is not excluded, however, that the change of nucleotide occupancy at catalytic β subunits at low [ATP] also contributes to the reversible transition of ε.

The position of the long pause of $\alpha_3\beta_3\gamma\varepsilon$ is at the 80°-position, in agreement with the case of cyanobacterial F_1 [18], suggesting that the conformational transition of ε is allowed only when the complex is at 80°-position. Since it has been known for $\alpha_3\beta_3\gamma$ that MgADP inhibition is responsible for the long pause at 80° [11], it is likely that the transition of ε is allowed only when $\alpha_3\beta_3\gamma\varepsilon$ is in the MgADP-inhibited state at low [ATP] where ε is free from ATP-dependent stabilization of the hairpin form (Fig. 4B). The model does not assume the enzyme species that is escaped from MgADP inhibition but is inhibited by extended ε. Indeed, if this species exists, active $\alpha_3\beta_3\gamma\varepsilon$ molecule with hairpin ε can decay via two pathways and its life-time should be shorter than that of $\alpha_3\beta_3\gamma$ that decays via a single pathway. Relation between ε and MgADP inhibition was also suggested [28] and confirmed experimentally for TF_oF_1 [29]. It seems worth testing whether the mutant $\alpha_3\beta_3\gamma\varepsilon$ resistant to MgADP inhibition is also resistant to inhibition by ε.

The manner of inhibition of F_1-ATPase by ε varies among species. At least there are two types: in one type, the inhibition is observed only at low [ATP], while in the other type, it is observed at

all [ATP]. The inhibition is reversible at low [ATP] in the former but actually irreversible in the latter at all [ATP]. TF_1 belongs to the former, and cyanobacterial F_1 and CF_1 belong to the latter [13,18]. Rotation of cyanobacterial F_1 stops completely and irreversibly by ε [18]. Most likely, EF_1 also belongs to the latter. ATPase of ε-less EF_1 was largely (80–90%) inhibited at all [ATP] by addition of excess ε [16] and apparent reversibility of inhibition is due to the dissociation of ε from EF_1. Time-averaged rate of rotation and steady-state ATPase activity of ε-containing EF_1 was reduced about 50% by addition of excess ε [15] and this incomplete, reversible inhibition is also probably due to the same reason. The difference between two types of ε inhibition can be originated from the ability of ε of TF_1 to bind ATP: at high [ATP], ATP binds and stabilizes the non-inhibitory hairpin conformation of ε of TF_1. The interaction of ε of EF_1 with ATP was detected but the affinity was very weak ($K_d \sim 20$ mM) [25]. It should be added that the affinity of ε of TF_1 is strong at 25 °C but would be weak ($K_d \sim 0.6$ mM) at 65 °C, a physiological temperature of *Bacillus* PS3 [26]. It is interesting to see the distribution of ε capable of ATP-binding and its physiological function in various organisms.

Appendix A. Supplementary data

Supplementary data associated with this article can be found, in the online version, at doi:10.1016/j.febslet.2009.02.038.

References

[1] Boyer, P.D. (1993) The binding change mechanism for ATP synthase – some probabilities and possibilities. Biochim. Biophys. Acta. 1140, 215–250.

[2] Senior, A.E. (2007) ATP synthase: motoring to the finish line. Cell 130, 220–221.

[3] Gibbons, C., Montgomery, M.G., Leslie, A.G. and Walker, J.E. (2000) The structure of the central stalk in bovine F_1-ATPase at 2.4 A resolution. Nat. Struct. Biol. 7, 1055–1061.

[4] Noji, H., Yasuda, R., Yoshida, M. and Kinosita Jr., K. (1997) Direct observation of the rotation of F_1-ATPase. Nature 386, 299–302.

[5] Yasuda, R., Noji, H., Yoshida, M., Kinosita Jr., K. and Itoh, H. (2001) Resolution of distinct rotational substeps by submillisecond kinetic analysis of F_1-ATPase. Nature 410, 898–904.

[6] Nishizaka, T., Oiwa, K., Noji, H., Kimura, S., Muneyuki, E., Yoshida, M. and Kinosita Jr., K. (2004) Chemomechanical coupling in F_1-ATPase revealed by simultaneous observation of nucleotide kinetics and rotation. Nat. Struct. Mol. Biol. 11, 142–148.

[7] Shimabukuro, K., Yasuda, R., Muneyuki, E., Hara, K.Y., Kinosita Jr., K. and Yoshida Jr., M. (2003) Catalysis and rotation of F_1 motor: cleavage of ATP at the catalytic site occurs in 1 ms before 40 degree substep rotation. Proc. Natl. Acad. Sci. USA 100, 14731–14736.

[8] Adachi, K., Oiwa, K., Nishizaka, T., Furuike, S., Noji, H., Itoh, H., Yoshida, M. and Kinosita Jr., K. (2007) Coupling of rotation and catalysis in F_1-ATPase revealed by single-molecule imaging and manipulation. Cell 130, 309–321.

[9] Minkov, I.B., Fitin, A.F., Vasilyeva, E.A. and Vinogradov, A.D. (1979) Mg^{2+}-induced ADP-dependent inhibition of the ATPase activity of beef heart mitochondrial coupling factor F_1. Biochem. Biophys. Res. Commun. 89, 1300–1306.

[10] Jault, J.M., Dou, C., Grodsky, N.B., Matsui, T., Yoshida, M. and Allison, W.S. (1996) The $\alpha_3\beta_3\gamma$ subcomplex of the F_1-ATPase from the thermophilic *Bacillus* PS3 with the β T165S substitution does not entrap inhibitory MgADP in a catalytic site during turnover. J. Biol. Chem. 271, 28818–28824.

[11] Hirono-Hara, Y., Noji, H., Nishiura, M., Muneyuki, E., Hara, K.Y., Yasuda, R., Kinosita Jr., K. and Yoshida Jr., M. (2001) Pause and rotation of F_1-ATPase during catalysis. Proc. Natl. Acad. Sci. USA 98, 13649–13654.

[12] Jault, J.M. and Allison, W.S. (1993) Slow binding of ATP to noncatalytic nucleotide binding sites which accelerates catalysis is responsible for apparent negativecooperativity exhibited by the bovine mitochondrial F_1-ATPase. J. Biol. Chem. 268, 1558–1566.

[13] Richter, M.L., Patrie, W.J. and McCarty, R.E. (1984) Preparation of the ε subunit and ε subunit-deficient chloroplast coupling factor 1 in reconstitutively active forms. J. Biol. Chem. 259, 7371–7373.

[14] Keis, S., Stocker, A., Dimroth, P. and Cook, G.M. (2006) Inhibition of ATP hydrolysis by thermoalkaliphilic F_1F_o-ATP synthase is controlled by the C terminus of the ε subunit. J. Bacteriol. 188, 3796–3804.

[15] Nakanishi-Matsui, M., Kashiwagi, S., Hosokawa, H., Cipriano, D.J., Dunn, S.D., Wada, Y. and Futai, M. (2006) Stochastic high-speed rotation of *Escherichia coli* ATP synthase F_1 sector: the ε subunit-sensitive rotation. J. Biol. Chem. 281, 4126–4131.

[16] Weber, J., Dunn, S.D. and Senior, A.E. (1999) Effect of the ε-subunit on nucleotide binding to *Escherichia coli* F_1-ATPase catalytic sites. J. Biol. Chem. 274, 19124–19128.

[17] Kato, Y., Matsui, T., Tanaka, N., Muneyuki, E., Hisabori, T. and Yoshida, M. (1997) Thermophilic F_1-ATPase is activated without dissociation of an endogenous inhibitor, ε subunit. J. Biol. Chem. 272, 24906–24912.

[18] Konno, H., Murakami-Fuse, T., Fujii, F., Koyama, F., Ueoka-Nakanishi, H., Pack, C.G., Kinjo, M. and Hisabori, T. (2006) The regulator of the F_1 motor: inhibition of rotation of cyanobacterial F_1-ATPase by the ε subunit. EMBO. J. 25, 4596–4604.

[19] Wilkens, S., Dahlquist, F.W., McIntosh, L.P., Donaldson, L.W. and Capaldi, R.A. (1995) Structural features of the ε subunit of the *Escherichia coli* ATP synthase determined by NMR spectroscopy. Nat. Struct. Biol. 2, 961–967.

[20] Zimmermann, B., Diez, M., Zarrabi, N., Graber, P. and Borsch, M. (2005) Movements of the ε-subunit during catalysis and activation in single membrane-bound H^+-ATP synthase. EMBO. J. 24, 2053–2063.

[21] Aggeler, R. and Capaldi, R.A. (1996) Nucleotide-dependent movement of the ε subunit between α and β subunits in the *Escherichia coli* F_1F_0-type ATPase. J. Biol. Chem. 271, 13888–13891.

[22] Rodgers, A.J. and Wilce, M.C. (2000) Structure of the γ–ε complex of ATP synthase. Nat. Struct. Biol. 7, 1051–1054.

[23] Suzuki, T., Murakami, T., Iino, R., Suzuki, J., Ono, S., Shirakihara, Y. and Yoshida, M. (2003) F_0F_1-ATPase/synthase is geared to the synthesis mode by conformational rearrangement of ε subunit in response to proton motive force and ADP/ATP balance. J. Biol. Chem. 278, 46840–46846.

[24] Kato-Yamada, Y. and Yoshida, M. (2003) Isolated ε subunit of thermophilic F_1-ATPase binds ATP. J. Biol. Chem. 278, 36013–36016.

[25] Yagi, H., Kajiwara, N., Tanaka, H., Tsukihara, T., Kato-Yamada, Y., Yoshida, M. and Akutsu, H. (2007) Structures of the thermophilic F_1-ATPase ε subunit suggesting ATP-regulated arm motion of its C-terminal domain in F_1. Proc. Natl. Acad. Sci. USA 104, 11233–11238.

[26] Iino, R., Murakami, T., Iizuka, S., Kato-Yamada, Y., Suzuki, T. and Yoshida, M. (2005) Real-time monitoring of conformational dynamics of the ε subunit in F_1-ATPase. J. Biol. Chem. 280, 40130–40134.

[27] Sakaki, N., Shimo-Kon, R., Adachi, K., Itoh, H., Furuike, S., Muneyuki, E., Yoshida, M. and Kinosita Jr., K. (2005) One rotary mechanism for F_1-ATPase over ATP concentrations from millimolar down to nanomolar. Biophys. J. 88, 2047–2056.

[28] Feniouk, B.A. and Junge, W. (2005) Regulation of the F_oF_1-ATP synthase: the conformation of subunit ε might be determined by directionality of subunit γ rotation. FEBS Lett. 579, 5114–5118.

[29] Feniouk, B.A., Suzuki, T. and Yoshida, M. (2007) Regulatory interplay between proton motive force, ADP, phosphate, and subunit ε in bacterial ATP synthase. J. Biol. Chem. 282, 764–772.